Superfluorescent transitions between high-lying levels in an external electric field

T. Becker and R.-H. Rinkleff
Abteilung Spektroskopie, Institut für Atom- und Molekülphysik, Universität Hannover, Appelstrasse 2, 3000 Hannover 1, Federal Republic of Germany
(Received 29 October 1990; revised manuscript received 12 February 1991)

The occurrence of superfluorescence in the near-infrared regime has been investigated between high-lying levels of Sr, Ba, and Na under the influence of a static homogeneous external electric field. The time inequalities for single-pulse superfluorescence were fulfilled. The measurements show for all the investigated superfluorescent transitions that the square root of the peak intensity of the superfluorescent pulse decreases with the square of the electric-field strength. If one takes into account the dependence of the number of excited atoms, the wavelengths, and the line strengths of the superfluorescent pulses on the electric-field strengths, the experimental findings cannot be explained by well-known theories of superfluorescence.

INTRODUCTION

Superfluorescence (SF) is a coherent spontaneous emission from an ensemble of atoms. Because of the long wavelengths and large dipole moments of transitions between high-lying levels, the decaying atoms may act cooperatively due to coupling by their common near-radiation field. SF resulting from this strong coupling was predicted by Dicke [1] in 1954, and experimentally confirmed in the optical region by Skribanowitz *et al.* [2] in 1973.

Some of the early theories considered pointlike samples, i.e., samples with all atoms contained in a volume with linear dimensions small compared to λ, the wavelength of the superfluorescent radiation. Pointlike samples, however, would require very special experimental configurations, and therefore subsequent theories treated extended samples, with all dimensions large compared to λ; in particular, samples that take the shape of a thin pencil. The SF radiation is characterized by the emission of a delayed pulse with peak intensity proportional to N^2, where N is the total number of atoms. In the pencil-shape geometry the radiation is emitted in a narrow cone in both directions along the sample axis.

For an unambiguous test of the theories it is desirable that experiments be performed on the simplest possible system and that they obey a set of conditions first formulated by Bonifacio and Lugiato [3] for the regime they denoted "pure SF." In this regime the population of the excited level in a pure two-level atom is removed by one superfluorescent pulse and not by ringing, i.e., by a sequence of superfluorescent pulses. Gibbs *et al.* [4] showed in their cesium experiment that single-pulse emission can be realized.

SF has been observed in the far-infrared [2,5,6], the near-infrared [7–9], and the visible regions [10,11]. It was shown [12–14] that it is possible to influence SF in a cavity. This is due to the fact that the collective emission in a cavity occurs only at transitions for which the cavity is resonant. Recently we have shown [15] that it is also possible to eliminate superfluorescent transitions between high-lying states of Sr by applying an external electric field. In this paper these measurements were extended, and it was found that for all the investigated superfluorescent transitions in Sr, Ba, and Na the square root of the maximum of the intensity of the superfluorescent pulse decreases with the square of the electric-field strength. Calculations were carried out for several theories of SF.

CONDITIONS FOR SUPERFLUORESCENCE

Simple experimental conditions make theoretical discussion of the results feasible; therefore, experiments should be performed with single superfluorescent pulses. The Bonifacio and Lugiato conditions for single-pulse SF [3] can be summarized by inequalities between times characterizing the experiment, i.e.,

$$\tau_E < \tau_C < \tau_R < \tau_D < T_1, T_2', T_2^* \ . \tag{1}$$

The sample transit or escape time is

$$\tau_E = L/c \ , \tag{2}$$

where L is the length of the pencil-shaped sample of inverted atoms. The Arecchi-Courtens cooperation time τ_c [16] is the maximum separation time between transitions of atoms decaying cooperatively, given by

$$\tau_C = \sqrt{\tau_E \tau_R} \ , \tag{3}$$

where the characteristic SF time τ_R [17],

$$\tau_R = \frac{8\pi\tau_0}{2n\lambda^2 L} \ , \tag{4}$$

depends on the partial lifetime of the excited level for the superfluorescent transition τ_0, the inversion density n, and the wavelength of the superfluorescent transition λ. The delay time τ_D between the creation of the inversion and the peak of the SF emission is typically 10 to 100 times longer than the characteristic SF time τ_R and is

easily measured. The relevant relaxation times are the inversion relaxation time T_1, the inhomogeneous relaxation time or dephasing time T_2^*, and the homogeneous relaxation time T_2'. One can calculate T_1 and T_2' from the radiative lifetimes. If one studies SF between an upper level $|a\rangle$ and a lower level $|b\rangle$, one has [18]

$$\frac{1}{T_1}=\frac{1}{\tau_{ab}}+\frac{1}{2\tau_{ac}}+\frac{1}{2\tau_{bd}} , \tag{5}$$

where τ_{ab} is the partial lifetime of $|a\rangle$ for the transition from $|a\rangle$ to $|b\rangle$ and τ_{ac} and τ_{bd} are the lifetimes of $|a\rangle$ and $|b\rangle$ to all other lower states. Similarly, the expression for T_2' is given by [18]

$$\frac{1}{T_2'}=\frac{1}{2}\left[\frac{1}{\tau_a}+\frac{1}{\tau_b}\right] , \tag{6}$$

where τ_a and τ_b are the radiative lifetimes of the two levels in question. T_2^* is usually determined by Doppler broadening [7]

$$T_2^*=\frac{3}{\Delta\omega_D} , \tag{7}$$

where $\Delta\omega_D$ is the full Doppler width at half maximum. Finally, one has to fulfill the condition

$$\tau_P<\tau_D , \tag{8}$$

where τ_P is the full width at half maximum of the exciting laser pulse. Equation (8) means that the inversion should be prepared in a time much shorter than the SF buildup time.

PRINCIPLE OF MEASUREMENTS

The experiments were designed to approach as closely as possible the desirable conditions for single-pulse SF summarized by Eq. (1). In particular, in order to lengthen the Doppler dephasing time T_2^*, we used an atomic beam instead of a cell. The basic elements of the experimental arrangement are shown in Fig. 1. The atomic beam was perpendicular to the direction of the electric field, which was produced by two Stark plates with 60-mm diameter and 10-mm separation. In the center between the Stark plates the atom-beam density was approximately 10^{10} cm^{-3}. The atoms were excited in a resonant two-step transition by two dye-laser pulses. The dye lasers were simultaneously pumped by an excimer laser and had a line width of 3 GHz. The pulse duration was 13 ns and the energy of the pulses about 1 mJ. In order to check Eq. (8), we changed the pump gas of the excimer laser from XeCl to N_2. The pulse duration was then less than 5 ns. The experimental results did not show a dependence on the pulse duration. To observe the SF in pure electric fields, the earth's magnetic field was compensated within 5×10^{-7} T by three pairs of Helmholtz coils.

The principle of excitation and observation is shown in a fictitious level diagram in Fig. 2. The atoms were excited stepwise via level 2 into level 3. Due to this excitation process, the atomic population was initially inverted for

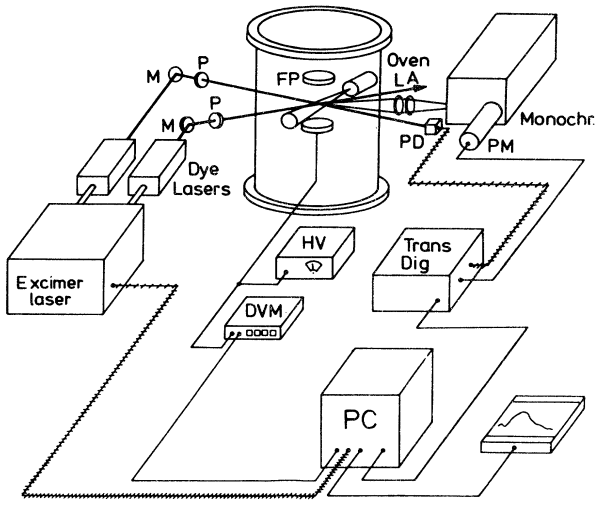

FIG. 1. Experimental setup. M, mirror; P, polarizer; A, analyzer; L, lens; FP, electric-field plates; PM, photomultiplier, PD, photodiode; Trans Dig, transient digitizer; HV, high-voltage power supply; DVM, digital voltmeter; PC, personal computer.

two allowed optical transitions, namely, $3\rightarrow4$ and $3\rightarrow5$. From theoretical results concerning SF it is known [19] that the transition with the shortest time constant τ_R causes the system to start radiating. In Fig. 2 the atoms thus radiate on transition $3\rightarrow4$ first, because this transition has the largest wavelength and consequently the shortest SF time [Eq. (4)]. Due to the differences in energy between high-lying states, the atoms emit by SF at infrared wavelengths. This emission process can be detected either directly, by monitoring the infrared intensity, or indirectly, as in the present experiment, by observing the fluorescence from the superfluorescently populated levels to lower states ($4\rightarrow7$ in Fig. 2). The fluorescence was detected by means of a monochromator and a high-speed photomultiplier. The single-shot signal was recorded time resolved by a fast transient digitizer, stored by a per-

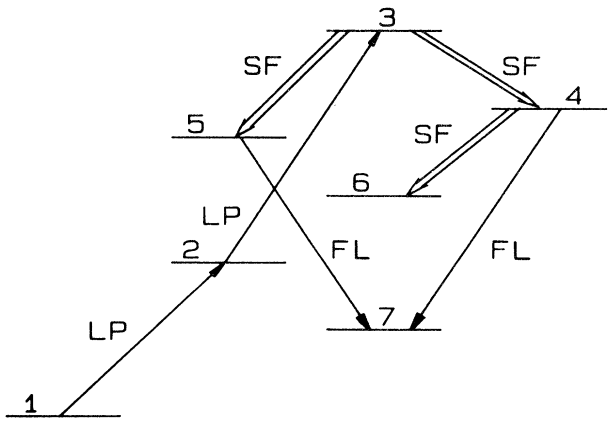

FIG. 2. Fictitious level diagram. LP, laser excitation pulse; SF, superfluorescent transition; FL, observed transition.

sonal computer, and subsequently analyzed. Each experimental run consisted of 500 single measurements, which were averaged to enhance the signal-to-noise ratio. An example of an averaged signal is shown in Fig. 3(a).

The connection between the SF pulse and the monitored signal can be expressed by a rate equation. The time dependence of the population density $n(t)$ of the superfluorescently populated level is given by

$$\frac{dn(t)}{dt} \propto -\frac{1}{\tau}n(t)+kI_{3\to4}(t) \ . \tag{9}$$

τ is the radiative lifetime of the superfluorescently populated level and can be determined from the exponential part of the decay curve [see Fig. 3(a)] by a least-squares-fit procedure. $I_{3\to4}(t)$ is the time dependence of the intensity of the superfluorescent pulse and k is a constant. Since the observed intensity $I_{4\to7}(t)$ is proportional to the population density of level 4, one gets

$$I_{3\to4}(t) \propto \frac{1}{\tau}I_{4\to7}(t)+\frac{dI_{4\to7}(t)}{dt} \ . \tag{10}$$

Thus it is possible to extract the SF intensity $I_{3\to4}(t)$ from the measured intensity $I_{4\to7}(t)$. Figure 3 shows an example of a measured intensity and the derived time dependence of the SF intensity.

The system begins to superfluoresce on the transition with the longest wavelength. If branching is possible, and the density is high enough, the atoms are able to emit by SF at several transitions ($3\to4$ and $3\to5$). This competing process occurs after the superfluorescent transition that starts the radiation. Cascade SF, i.e., superfluorescent emission between sequential transitions ($3\to4$, $4\to6$), is also known. Cascading can occur when the population buildup in the lower level of the initial SF transition is sufficiently large to produce high gain at the coupled sequential transition. A detailed study of this effect has been carried out by Crubellier *et al.* [9].

In order to investigate the behavior of SF in an electric field, one has to do the measurements on a system that is as simple as possible, since the different theories of SF assume only a two-level system. In our measurements, competition as well as cascade effects were therefore avoided.

EVIDENCE OF SUPERFLUORESCENCE

In order to check the superfluorescent character of the emission, the variation of pulse height, pulse width, and delay was studied. From theoretical results about SF it is known (e.g., [3], [20], and [21]) that the intensity distribution of the SF pulse is given by

$$I(t)=I_M \operatorname{sech}^2\left[\frac{t-\tau_D}{2\tau_R}\right] \tag{11}$$

and that the peak intensity I_M is proportional to N^2, the total number of atoms. In contrast to this, the delay time τ_D and the pulse width are proportional to N^{-1}. To test these dependences, time-resolved recordings were performed for different atomic-beam densities. As an exam-

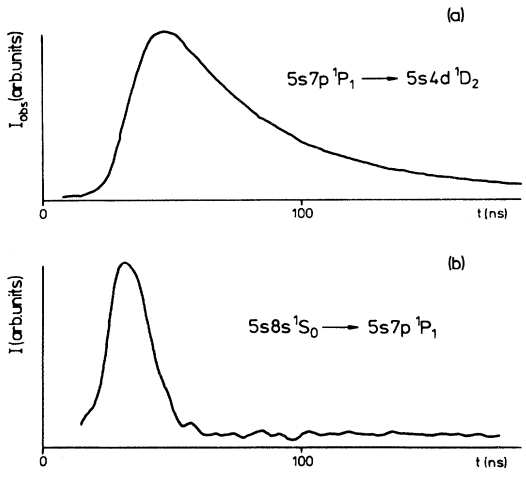

FIG. 3. (a) Observed decay curve for the superfluorescently populated $5s7p\ ^1P_1$ level; (b) the superfluorescent pulse derived from this decay curve.

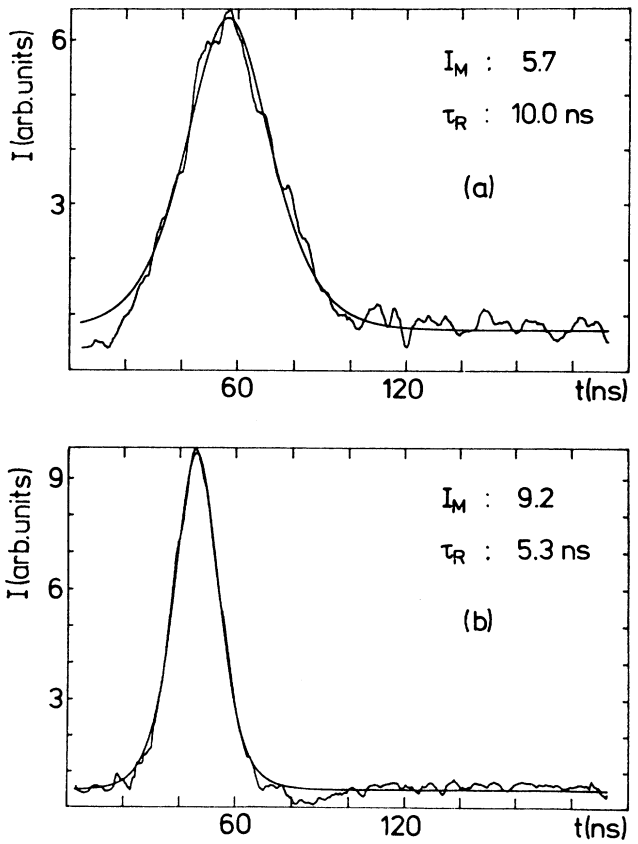

FIG. 4. SF pulse for two different atomic densities for the transition $6s8p\ ^1P_1-6p^2\ ^3P_0$ in barium. Oven temperature (a) $T=870$ K, (b) $T=940$ K.

ple, Fig. 4 shows two SF signals of the transition $6s8p\ ^1P_1-6p^2\ ^3P_0$ in Ba for different atomic-beam densities. The typical shape of the single symmetric pulse was found. At the experimental pulse shapes a theoretical pulse (11) was fitted with the delay time τ_D, SF time τ_R, and peak intensity I_M as free parameters. Figure 4 shows good agreement between experimental and theoretical curves. On increasing the density, one can see that the peak intensity increases, but that the delay time and the pulse width decrease.

Another method of showing the superfluorescent population of a level is to monitor the dependence of the fluorescent spectrum on increasing atomic-beam density. As an example, Fig. 5 shows three transitions of Na (see Fig. 6) as a function of increasing atomic density. For these measurements the atoms were excited via the $3p\ ^2P_{3/2}$ into the $7s\ ^2S_{1/2}$ level by two pulsed dye lasers. The monochromator was scanned and the signals were recorded by the transient digitizer and stored by the computer. By scanning the monochromator over a range of 50 nm, we stored several thousand shots. Subsequently, the intensity data of several shots were added up to enhance the signal-to-noise ratio. By this process we simulate a boxcar integrator, with the advantage that we can choose the timing afterwards.

The monochromator was scanned from 470 to 520 nm, so that, according to Fig. 6, three transitions are expected. When the temperature of the atomic-beam oven is increased by 45 K, the signals on the left and on the right (475 and 515 nm) increase by a factor of 2, whereas the signal in the middle (498 nm) increases by a factor of 4. This provides evidence that the signal in the middle comes from a level that was populated by SF, because the intensity of the SF pulse goes as N^2 in contrast to the normal fluorescence, which goes as N.

Finally, we have to show that the electric field acts only on the SF transition and not on the normal optical transition. This is demonstrated in Fig. 7, which shows the same three transitions in Na as Fig. 5. When the electric-field strength is increased, the middle signal decreases by a factor of 2, whereas the other transitions, which start from levels not populated by SF, do not change their intensity.

EXPERIMENTAL RESULTS

Strontium

A partial level diagram of Sr is shown in Fig. 8. The atoms were excited stepwise via the $5s5p\ ^1P_1$ level into

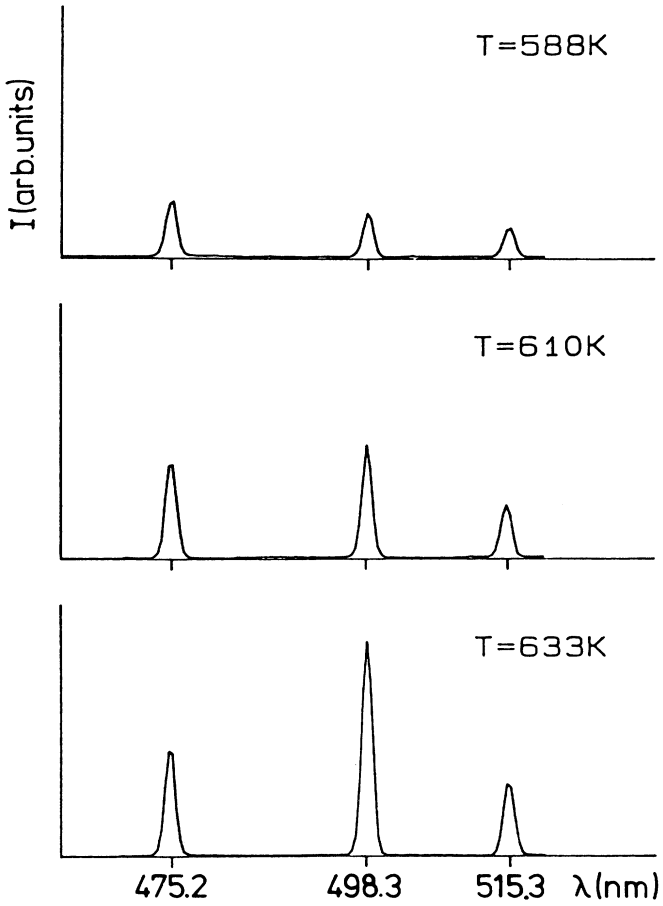

FIG. 5. Fluorescence spectra of Na for different atomic-beam densities. T, oven temperature; excited level $7s\ ^2S_{1/2}$. Transitions: see Fig. 6.

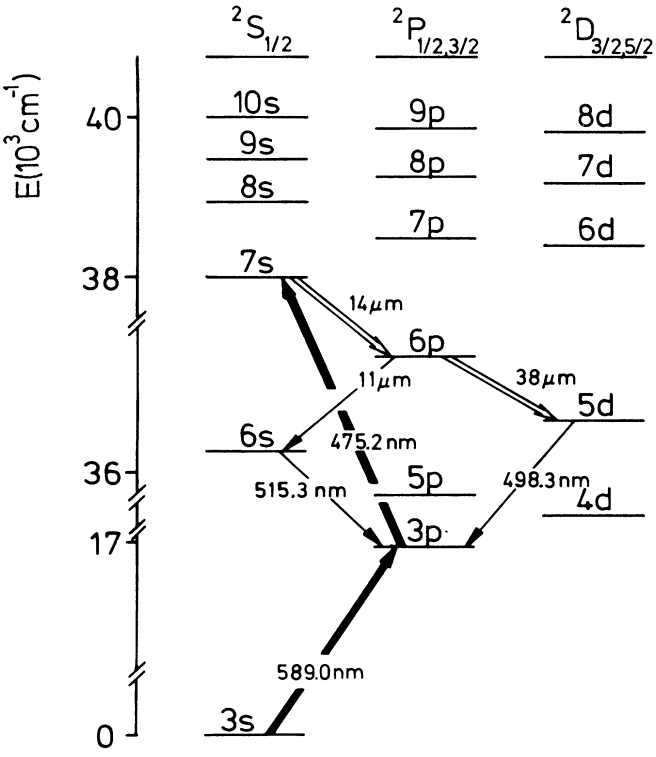

FIG. 6. Na energy levels relevant for the measurements. ➡, laser excitation pulse; ⟹, SF pulse; →, observed fluorescence light.

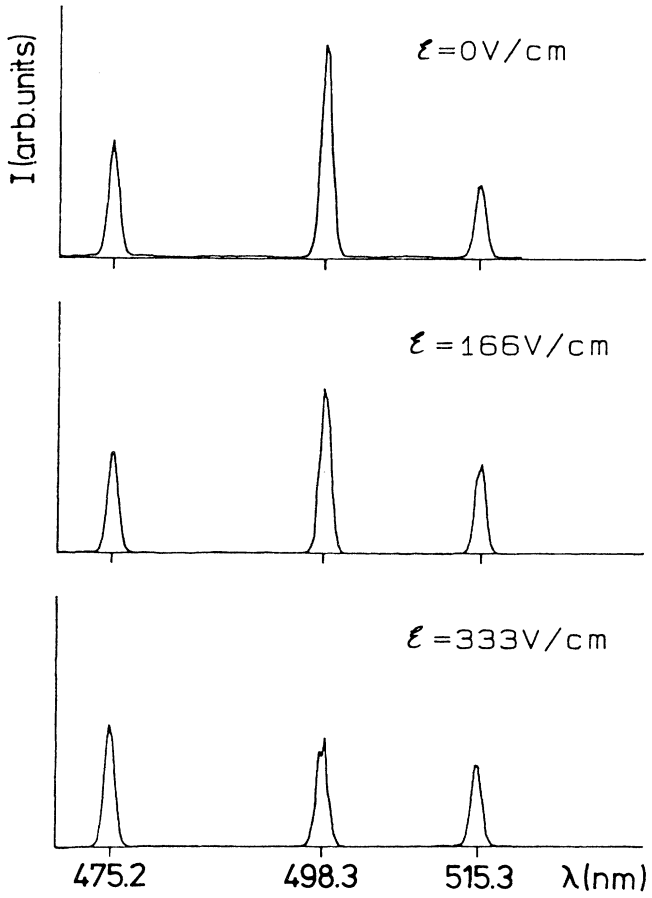

FIG. 7. Fluorescence spectra of Na for different electric-field strengths $\mathcal{E}$. Transitions; see Fig. 6.

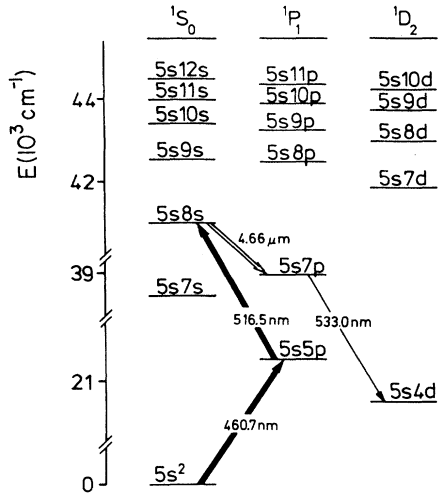

FIG. 8. Sr energy levels relevant for the measurements. ⟹, laser excitation pulse; ⟹, SF pulse; →, observed fluorescence light.

the $5sns\ ^1S_0$ level with $n=8-12$. The existence of superfluorescent decays to the $5s(n-1)p\ ^1P_1$ levels was proved by observing the population transfer to the $5s4d\ ^1D_2$ state. If the atomic density is sufficiently small, no superfluorescent cascades were observed.

The important times for SF are listed in Table I. It can be seen that the Bonifacio and Lugiato time inequalities for single-pulse SF (1) are fulfilled. The radiative lifetimes of the $5snp\ ^1P_1$ levels were taken from Ref. [23] and of the $5sns\ ^1S_0$ levels from Ref. [22], except for the lifetime of the $5s12s\ ^1S_0$ level, which was determined in this work. The partial lifetimes, which are equal to the reciprocal Einstein A factors for the transitions, were calculated in Coulomb approximation [24,25] and the other times are given by the experimental conditions [26].

As an example of the measurements, Fig. 9 shows the observed intensity of the transition $5s7p\ ^1P_1 \rightarrow 5s4d\ ^1D_2$. The maximum of the intensity of the SF pulse was derived using (10) and (11). In Fig. 10 the square root of the peak intensity was plotted against the square of the electric-field strength $\mathcal{E}$ for three investigated transitions. For each transition the measured points are on a straight line. The solid line was obtained by a least-squares-fit procedure. This linear dependence was found for all the measured single-pulse superfluorescent transitions. The gradients of the function relating $\sqrt{I_M(\mathcal{E})/I_M(\mathcal{E}=0)}$ to $\mathcal{E}^2$ are listed in Table II, and are discussed later.

Barium

A partial level diagram of Ba is shown in Fig. 11. The atoms were excited stepwise via the $6s6p\ ^1P_1$ level into the $6sns\ ^1S_0$ levels ($n=10,11$), into the $6sn'd\ ^1D_2$ levels ($n'=9-11$), and into the level $6p^2\ ^1D_2$. The SF occurs from the $6sns\ ^1S_0$ levels to the nearest lower $^1P_1$ level, from the $6sn'd\ ^1D_2$ levels to the $6s(n'-3)f\ ^1F_3$ levels,

TABLE I. Important times for the measured Sr transitions; λ in μm, all times (see text) in ns.

SF transition	λ	$\tau(^1S_0)$	$\tau(^1P_1)$	τ_E	τ_C	τ_R	T_1	T_2'	T_2^*
$5s8s\ ^1S_0 \rightarrow 5s7p\ ^1P_1$	4.66	70.9[a]	39.2[b]	0.03	0.34	3.83	46.5	50.5	37.6
$5s9s\ ^1S_0 \rightarrow 5s8p\ ^1P_1$	74.82	119.0[a]	27.1[b]	0.03	0.27	2.40	44.1	44.1	507.0
$5s10s\ ^1S_0 \rightarrow 5s9p\ ^1P_1$	54.32	303.0[a]	42.7[b]	0.03	0.22	1.68	74.7	74.9	368.6
$5s11s\ ^1S_0 \rightarrow 5s10p\ ^1P_1$	62.30	376.0[a]	81.0[b]	0.03	0.17	1.00	132.6	133.3	422.7
$5s12s\ ^1S_0 \rightarrow 5s11p\ ^1P_1$	79.11	889.0	123.0[b]	0.03	0.20	1.36	218.4	219.2	536.8

[a]Reference [22].
[b]Reference [23].

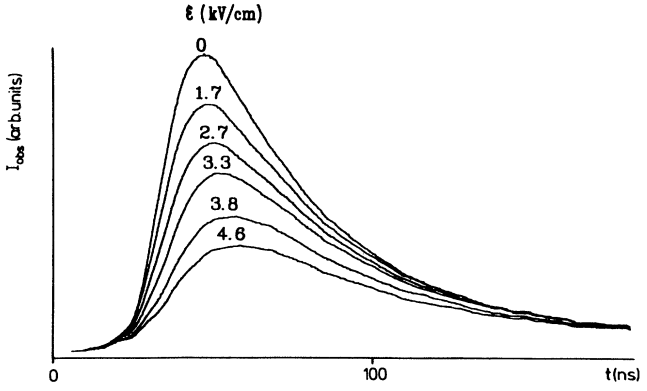

FIG. 9. Observed decay curves from the superfluorescently populated level $5s7p\ ^1P_1$ following laser excitation of the $5s8s\ ^1S_0$ level for different electric-field strengths. Signals observed in the transition $5s7p\ ^1P_1-5s4d\ ^1D_2$.

and from the $6p^2\ ^1D_2$ level to the $6s9p\ ^1P_1$ level. All the superfluorescent transitions were proved to exist by the presence of optical transitions to the $6s5d\ ^1D_2$ level. The time inequalities for single-pulse SF (1) were again fulfilled [26]. Superfluorescent cascades from the $^1S_0$ levels and superfluorescent competing transitions from the $^1D_2$ levels could be avoided if the atomic-beam density was sufficiently small, but in the latter case superfluorescent cascades could not be suppressed. As an example, Fig. 12(a) shows the intensity of the SF pulse of the transition $6s11d\ ^1D_2\rightarrow 6s8f\ ^1F_3$. The minimum indicates that the superfluorescently populated $6s8f\ ^1F_3$ level decays by a further SF pulse. The intensity distribution of Fig. 12(a) is given by

$$I(t)=I_{M1}\,\mathrm{sech}^2\left[\frac{t-\tau_{D1}}{2\tau_{R1}}\right]-I_{M2}\,\mathrm{sech}^2\left[\frac{t-\tau_{D2}}{2\tau_{R2}}\right]. \quad (12)$$

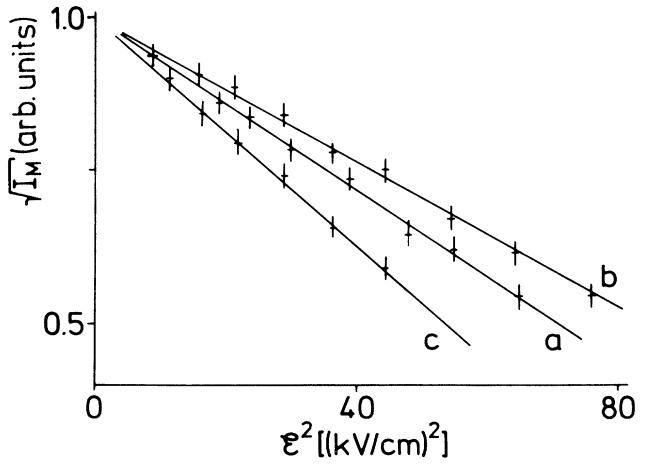

FIG. 10. Square root of the maxima of the intensity of the superfluorescent pulses plotted against the squared electric-field strengths for the Sr transitions (a) $5s8s\ ^1S_0-5s7p\ ^1P_1$, (b) $5s11s\ ^1S_0-5s10p\ ^1P_1$, (c) $5s12s\ ^1S_0-5s11p\ ^1P_1$.

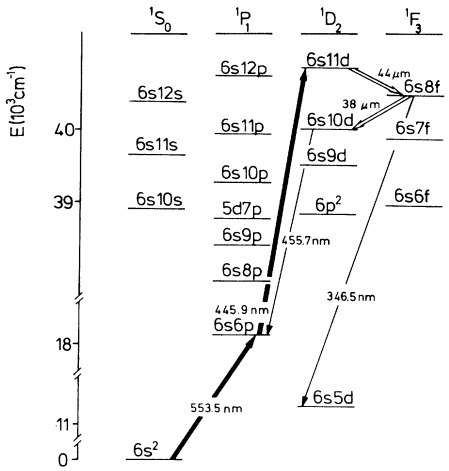

FIG. 11. Ba energy levels relevant for the measurements. ⟹, laser excitation pulse; ⟹, superfluorescent pulse; →, observed fluorescence light.

The second pulse can be suppressed by a small electric-field strength [Fig. 12(b)], as is also shown in Fig. 13. Figure 13(a) shows the dependence on the electric field of the fluorescence intensity from the laser populated level $6s11d\ ^1D_2$ observed in the transition $6s11d\ ^1D_2-6s6p\ ^1P_1$. Figure 13(b) shows the fluorescence intensity from the superfluorescently populated level $6s8f\ ^1F_3$ following laser excitation of the $6s11d\ ^1D_2$ level at the same three electric-field strengths. The signals were observed in the transition $6s8f\ ^1F_3-6s5d\ ^1D_2$. In Fig. 13(c) the fluorescence intensity from the level $6s10d\ ^1D_2$ is shown in the transition $6s10d\ ^1D_2-6s6p\ ^1P_1$. This level was populated by a superfluorescent cascade, which consists of two superfluorescent pulses: the first populates the $6s8f\ ^1F_3$ level and the second the $6s10d\ ^1D_2$ level. As a result of the electric-field strength of 170 V/cm, the second pulse in the SF cascade was suppressed [Fig. 13(c)], the population of the $6s8f\ ^1F_3$ level was a little lower than for 0 V/cm [Fig. 13(b)], and the intensity of the transition $6s11d\ ^1D_2-6s6p\ ^1P_1$ was increased [Fig. 13(a)]. Raising the field strength to 500 V/cm caused the superfluorescent pulse from the laser-excited $6s11d\ ^1D_2$ level to the $6s8f\ ^1F_3$ level to disappear [Fig. 13(b)], and caused the intensity in the transition $6s11d\ ^1D_2-6s6p\ ^1P_1$ to increase further [Fig. 13(a)].

Finally, if the electric-field strength was high enough to suppress the second superfluorescent pulse in a cascade, then plots of the square root of the peak intensity of the SF pulse versus the square of the electric-field strength show the same linear behavior as for Sr [26]. The gradients of the function relating $\sqrt{I_M(\mathcal{E})/I_M(\mathcal{E}=0)}$ and $\mathcal{E}^2$ are given in Table II.

Sodium

A partial level diagram of Na is shown in Fig. 6. The atoms were excited via the $3p\ ^2P_{3/2}$ level into the $ns\ ^2S_{1/2}$

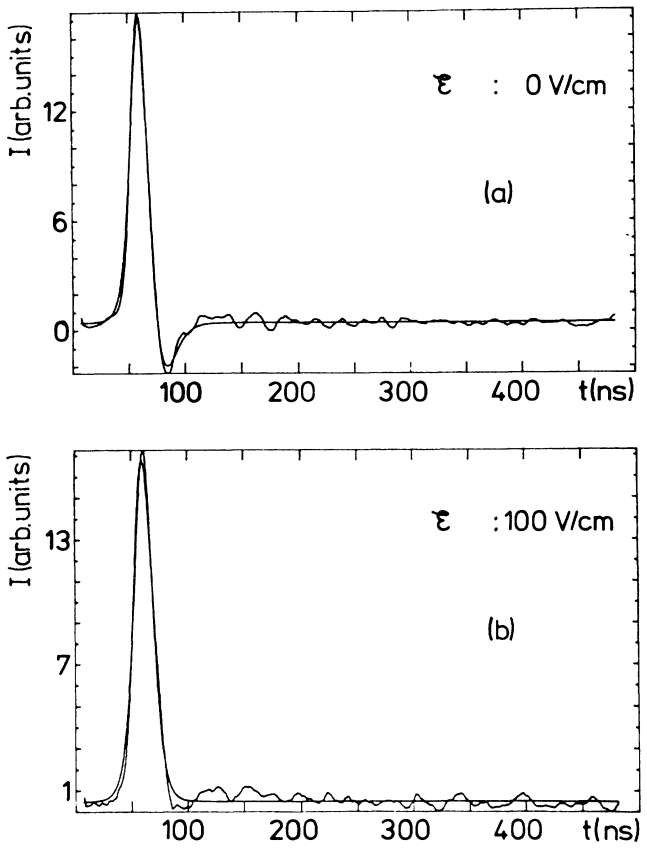

FIG. 12. Superfluorescent pulse of the Ba transition $6s11d\ ^1D_2-6s8f\ ^1F_3$ derived from the observed transition $6s8f\ ^1F_3-6s5d\ ^1D_2$ for different electric-field strengths (a) with and (b) without a superfluorescent cascade. The cascade consists of two pulses: The first one populates the $6s8f\ ^1F_3$ level and the second one depopulates this level.

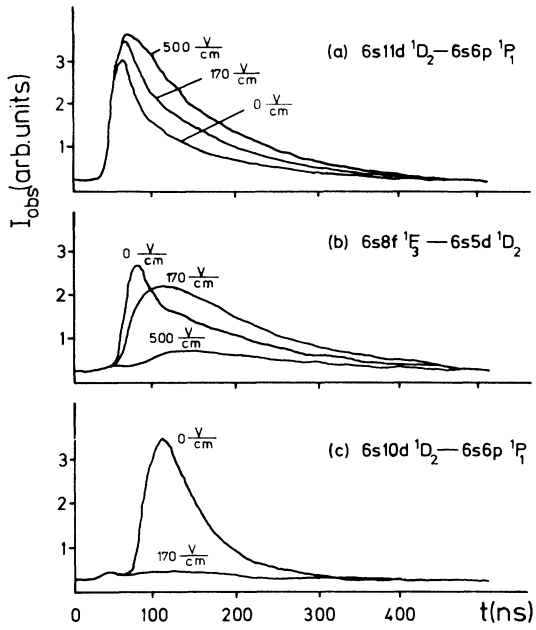

FIG. 13 Observed decay curves of Ba transitions for different electric-field strengths from (a) the laser-excited $6s11d\ ^1D_2$ level, (b) the superfluorescently populated $6s8f\ ^1F_3$ level, and (c) the level populated by a superfluorescent cascade, from the laser-excited $6s11d\ ^1D_2$ level via the $6s8f\ ^1F_3$ level.

levels with $n=6-9$. The time inequalities for single-pulse SF (1) were again fulfilled [26]. We found that superfluorescent cascades populate the $(n-2)d\ ^2D_J$ levels via the $(n-1)p\ ^2P_{J'}$ levels. In contrast to the measurements on Ba, it was not possible to suppress the second superradiant pulse relative to the first superfluorescent pulse in the cascades at lower electric-field strengths. Therefore, to have definite conditions in the measurements the $np\ ^2P_J$ levels ($n=5-8$) were directly excited from the ground state by a frequency-doubled dye laser. The fluorescence from the superradiantly populated $(n-1)d\ ^2D_{J'}$ levels was observed in the transitions to the $3p\ ^2P_{J''}$ levels. The dependence of the maximum intensity of the superradiant pulse on the electric-field strength was the same as for the alkaline-earth metals. The gradients of the function relating $\sqrt{I_M(\mathcal{E})/I_M(\mathcal{E}=0)}$ to $\mathcal{E}^2$ are again listed in Table II.

DISCUSSION

For discussion of the experimental results we study first the influence of the Stark splitting of the initial and final levels involved in superfluorescent transitions. An electric field splits degenerate levels into sublevels, and therefore the dipole moments on various nearly degenerate transitions oscillate at slightly different frequencies. For this reason phase coherence can be lost, and consequently the intensity of the superfluorescent pulse can be reduced. In all superfluorescent transitions studied, at least one of the levels is degenerate. If the Stark splitting were a possible explanation of the experimental findings, then the gradient m of the function relating $\sqrt{I_M(\mathcal{E})/I_M(\mathcal{E}=0)}$ and $\mathcal{E}^2$ should show a linear dependence on the Stark parameter α_2, which describes the Stark splitting. Such a correlation was not found. The values of m and α_2 of the investigated transitions in Sr and Ba are given in Table III. Thus we conclude that the lifting of the degeneracy cannot explain the experimental findings.

This conclusion is supported by an experiment in which the superfluorescent transitions were investigated under the influence of static homogeneous external magnetic field. Since the Zeeman splitting is proportional to the magnetic field B, one expects the square root of the peak intensity of the superfluorescent pulse to decrease linearly with the magnetic-field strength. Figure 14 shows the results for two superfluorescent transitions, one in Sr ($5s11s\ ^1S_0-5s10p\ ^1P_1$) and one in Ba ($6s11d\ ^1D_2-6s8f\ ^1F_3$). In the latter case the laser light was linearly polarized parallel to the magnetic field, so that only $\Delta m=0$ transitions were induced, as was done in the investigations in electric fields. No dependence of the

TABLE II. Comparison between experimental and theoretical values of the gradient m of the function $\sqrt{I_M(\mathcal{E})/I_M(\mathcal{E}=0)}=1+m\rho^2\mathcal{E}^2$ for all measured SF transitions; $\mathcal{E}$ in kV/cm, $\rho=1/(\text{kV/cm})$.

SF transition	Calculated (a)	Calculated (b)	Calculated (c)	Experimental
Sr $5s8s\ ^1S_0\rightarrow 5s7p\ ^1P_1$	$+3.0\times10^{-7}$	$+2.7\times10^{-7}$	$+5.1\times10^{-7}$	-7.0×10^{-3}
Sr $5s9s\ ^1S_0\rightarrow 5s8p\ ^1P_1$	-8.9×10^{-5}	-1.2×10^{-4}	-2.9×10^{-4}	-2.9×10^{-2}
Sr $5s10s\ ^1S_0\rightarrow 5s9p\ ^1P_1$	$+1.5\times10^{-5}$	-6.3×10^{-6}	-2.0×10^{-5}	-3.6×10^{-2}
Sr $5s11s\ ^1S_0\rightarrow 5s10p\ ^1P_1$	$+2.8\times10^{-4}$	$+2.5\times10^{-4}$	$+4.9\times10^{-4}$	-5.9×10^{-3}
Sr $5s12s\ ^1S_0\rightarrow 5s11p\ ^1P_1$	$+1.0\times10^{-3}$	$+1.1\times10^{-3}$	$+2.0\times10^{-3}$	-9.3×10^{-3}
Ba $6s10s\ ^1S_0\rightarrow 5d7p\ ^1P_1$	-2.6×10^{-4}	-2.2×10^{-4}	-4.6×10^{-4}	-8.0×10^{-2}
Ba $6s11s\ ^1S_0\rightarrow 6s10p\ ^1P_1$	-2.5×10^{-3}	-5.9×10^{-4}	-1.6×10^{-3}	-4.0×10^{-2}
Ba $6p^2\ ^1D_2\rightarrow 6s9p\ ^1P_1$	-1.4×10^{-4}	-1.3×10^{-4}	-2.7×10^{-4}	-1.0×10^{-2}
Ba $6s9d\ ^1D_2\rightarrow 6s6f\ ^1F_3$	-2.1×10^{-4}	-2.0×10^{-4}	-8.0×10^{-4}	-2.4×10^{-1}
Ba $6s10d\ ^1D_2\rightarrow 6s7f\ ^1F_3$	-3.2×10^{-3}	-5.0×10^{-3}	-6.3×10^{-3}	-8.0×10^{-1}
Ba $6s11d\ ^1D_2\rightarrow 6s8f\ ^1F_3$	-3.6×10^{-3}	-3.7×10^{-3}	-7.3×10^{-3}	-2.9×10^{-1}
Na $5p\ ^2P_{3/2}\rightarrow 4d\ ^2D_{5/2}$	-1.0×10^{-4}	-1.1×10^{-4}	-2.0×10^{-4}	-2.0×10^{-1}
Na $6p\ ^2P_{3/2}\rightarrow 5d\ ^2D_{5/2}$	-1.1×10^{-3}	-1.1×10^{-3}	-2.1×10^{-3}	-1.1×10^{-2}
Na $7p\ ^2P_{3/2}\rightarrow 6d\ ^2D_{5/2}$	-7.4×10^{-3}	-7.3×10^{-3}	-1.4×10^{-2}	-1.0×10^{-2}
Na $8p\ ^2P_{3/2}\rightarrow 7d\ ^2D_{5/2}$	-7.6×10^{-4}	-1.0×10^{-3}	-5.5×10^{-4}	-1.4×10^{-2}

[a]Calculated according to Eq. (13a).
[b]Calculated according to Eq. (13b).
[c]Calculated according to Eq. (13c).

peak intensity of the superfluorescent pulses on the magnetic-field strength was found. Thus it follows that the lift of the degeneracy does not play a dominant part in the explanation of the experimental results. This behavior can be explained if we assume that in our experiments there was only a single superfluorescent pulse between two particular sublevels and not a superposition of superfluorescent pulses of various nearly degenerate transitions that oscillate at different frequencies and mutually influence each other.

We now have to discuss other reasons for the dependence of the peak intensity of the superfluorescent pulse on the electric-field strength. To do this, we calculate the peak intensity according to different theories:

$$I_M \propto \begin{cases} \dfrac{SN^2}{\lambda^3}, & \text{Rehler and Eberly [20]} \quad (13a) \\ \dfrac{SN^2}{\lambda^2}, & \text{Bonifacio and Lugiato [3]} \quad (13b) \\ \dfrac{S^2N^2}{\lambda^3}, & \text{mean-field model without damping [27] .} \quad (13c) \end{cases}$$

Here, N is the number of atoms in the excited state, S the line strength, and λ the wavelength of the transition. S, N, and λ depend on the electric-field strength. Under the

TABLE III. Experimental values of the gradient m of the function $\sqrt{I_M(\mathcal{E})/I_M(\mathcal{E}=0)}=1+m\rho^2\mathcal{E}^2$ of measured superfluorescent transitions and values of the tensor polarizabilities α_2. α_2 in kHz/(V/cm)^2, $\mathcal{E}$ in kV/cm, and $\rho=1/(kV/cm)$.

Transitions	m	$\alpha_2(^1P_1)$	$\alpha_2(^1F_3)$
Sr $5s8s\ ^1S_0\rightarrow 5s7p\ ^1P_1$	-0.007	0.009	
Sr $5s9s\ ^1S_0\rightarrow 5s8p\ ^1P_1$	-0.029	-0.17	
Sr $5s10s\ ^1S_0\rightarrow 5s9p\ ^1P_1$	-0.036	-0.19	
Sr $5s11s\ ^1S_0\rightarrow 5s10p\ ^1P_1$	-0.0059	-0.30	
Sr $5s12s\ ^1S_0\rightarrow 5s11p\ ^1P_1$	-0.0093	-0.54	
Ba $6s10s\ ^1S_0\rightarrow 5d7p\ ^1P_1$	-0.08	-0.033	
Ba $6s11s\ ^1S_0\rightarrow 6s10p\ ^1P_1$	-0.04	-0.21	
Ba $6p^2\ ^1D_2\rightarrow 6s9p\ ^1P_1$	-0.01	0.12	
Ba $6s9d\ ^1D_2\rightarrow 6s6f\ ^1F_3$	-0.24		-0.18
Ba $6s10d\ ^1D_2\rightarrow 6s7f\ ^1F_3$	-0.80		-0.49
Ba $6s11d\ ^1D_2\rightarrow 6s8f\ ^1F_3$	-0.29		-0.37

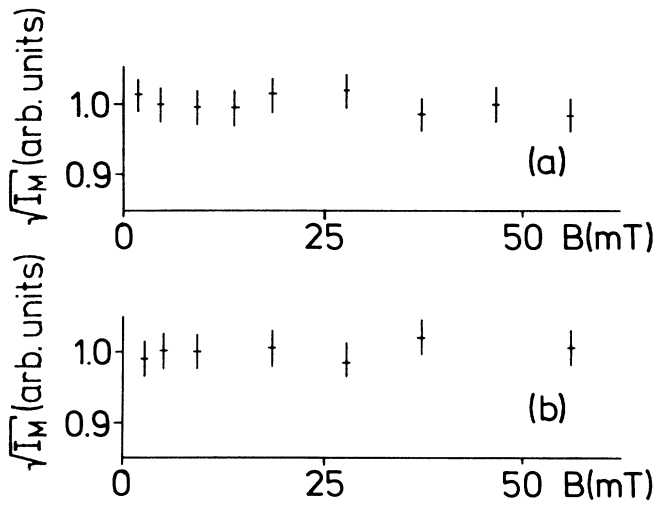

FIG. 14. Square root of the maxima of the intensity of the superfluorescent pulses plotted against the magnetic-field strengths B, (a) for the transition $5s11s\ ^1S_0-5s10p\ ^1P_1$ in Sr and (b) for the transition $6s11d\ ^1D_2-6s8f\ ^1F_3$ in Ba.

condition for large damping, the mean-field model with damping [6] shows the same dependence on the electric field as the model of Rehler and Eberly. In our experiments we had large damping, since all the measured superfluorescent pulses could be fitted with a sech^2 function (see, e.g., Figs. 4 and 12).

To study the dependence of the wavelength on the electric field, the Stark effect of the two levels that are connected by the superfluorescent pulse has to be calculated. The energy shift $\Delta W(JM)$ of a fine-structure level $|JM\rangle$ of a free atom exposed to an electric field $\mathcal{E}$ is given by [28,29]

$$\Delta W(JM)=-\left[\alpha_0(J)+\alpha_2(J)\frac{3M^2-J(J+1)}{J(2J-1)}\right]\frac{\mathcal{E}^2}{2}\ . \tag{14}$$

α_0 is the scalar polarizability describing the overall shift and α_2 is the tensor polarizability responsible for the splitting into the sublevels. α_0 and α_2 are given by

$$\alpha_0(J)=-\frac{2}{3(2J+1)}\sum_{\gamma',J'}\frac{|\langle\gamma J\|D^1\|\gamma'J'\rangle|^2}{E(\gamma J)-E(\gamma'J')}\ , \tag{15}$$

$$\alpha_2(J)=-4\left[\frac{5}{6}\frac{J(2J-1)}{(2J+3)(2J+1)(J+1)}\right]^{1/2}\times\sum_{\gamma',J'}(-1)^{J+J'}\times\frac{|\langle\gamma J\|D^1\|\gamma'J'\rangle|^2}{E(\gamma J)-E(\gamma'J')}\begin{Bmatrix}J & J' & 1\\ 1 & 2 & J\end{Bmatrix}, \tag{16}$$

where $\langle\gamma J\|D^1\|\gamma'J'\rangle$ is the reduced matrix element of the electric dipole operator D^1 connecting the levels $|\gamma J\rangle$ and $|\gamma'J'\rangle$ and $E(\gamma J)-E(\gamma'J')$ is the corresponding energy difference. The sum has to be extended over all the states $|\gamma'J'\rangle$ connected with the investigated state by the electric dipole operator. The sum converges so rapidly that the nearest 40 levels already make up more than 99% of the polarizability that is obtained by taking into account a much larger number of levels. The reduced matrix elements were calculated using the Coulomb approximation. The energy differences for the Sr levels were taken from Refs. [30–34], for the Ba levels from Refs. [35–38], and for the Na levels from Ref. [39].

Using the calculated polarizabilities, the Stark shift of the levels that are connected by an SF pulse were calculated with (14) in order to get the dependence of the wavelength on the electric field. The line strength is given by

$$S=|\langle\gamma J\|D^1\|\gamma'J'\rangle|^2\ . \tag{17}$$

Since the electric field admixes eigenstates of different parity, one has to use the perturbed wave functions, which are written as

$$|\gamma J\rangle=\frac{1}{N}\left[|\overline{\gamma J}\rangle+\sum_i\varepsilon_i|\overline{\gamma_i J'}\rangle+\sum_k[\beta_k|\overline{\gamma_k J''}\rangle+\beta'_k|\overline{\gamma_k(J''+1)}\rangle]\right] \tag{18}$$

with

$$N=\left[1+\sum_i\varepsilon_i^2+\sum_k(\beta_k^2+\beta_k'^2)\right]^{1/2},$$

$$\varepsilon_i=\frac{\langle\overline{\gamma_i J'}\|D^1\mathcal{E}\|\overline{\gamma J}\rangle}{E(\gamma J)-E(\gamma_i J')}\ ,$$

$$\beta_k=\frac{\langle\overline{\gamma_k J''}\|D^1\mathcal{E}\|\overline{\gamma J}\rangle}{E(\gamma J)-E(\gamma_k J'')}\ ,$$

$$\beta'_k=\frac{\langle\overline{\gamma_k(J''+1)}\|D^1\mathcal{E}\|\overline{\gamma J}\rangle}{E(\gamma J)-E[\gamma_k(J''+1)]}\ .$$

For Na, the wave functions, which are indicated by a horizontal bar, are pure configuration basis vectors. For a $^2P_{3/2}$ level, the perturbed wavefunction is given by (18) with $|\overline{\gamma_i J'}\rangle=|is\ ^2S_{1/2}\rangle$, $|\overline{\gamma_k J''}\rangle=|kd\ ^2D_{3/2}\rangle$, and $|\overline{\gamma_k(J''+1)}\rangle=|kd\ ^2D_{5/2}\rangle$. For Sr and Ba we used multiconfiguration wave functions, again indicated by a horizontal bar, derived from mixing parameters given by Refs. [31,34–36,40].

The line strengths in an electric field were derived by (17) using the perturbed wave functions (18), whereas the radial parts of the matrix elements were calculated by the Coulomb approximation. Equation (18) shows that the main contributions to the perturbed wave functions are given by the levels nearest to the state under consideration. Therefore, we restricted our calculations to the nearest states of each series.

The number of excited atoms N is proportional to the line strength of the laser transition:

$$N\propto|\langle\gamma J\|D^1\|\gamma'J'\rangle|^2\ . \tag{19}$$

These line strengths were also calculated with the per-

TABLE IV. Dependence of the wavelength, line strength, and number of excited atoms on the electric-field strength for the measured single-pulse superfluorescent transitions in Sr standardized to the case without the electric field [$\mathcal{E}$ in kV/cm, $\rho=1/(kV/cm)$].

SF transition	$\lambda(\mathcal{E})/\lambda(\mathcal{E}=0)$	$S_{JJ'}(\mathcal{E})/S_{JJ'}(\mathcal{E}=0)$	$N(\mathcal{E})/N(\mathcal{E}=0)$
$5s8s\ ^1S_0 \rightarrow 5s7p\ ^1P_1$	$1+0.18\times10^{-6}\rho^2\mathcal{E}^2$	$1+0.42\times10^{-6}\rho^2\mathcal{E}^2$	$1-0.24\times10^{-7}\rho^2\mathcal{E}^2$
$5s9s\ ^1S_0 \rightarrow 5s8p\ ^1P_1$	$1-0.15\times10^{-3}\rho^2\mathcal{E}^2$	$1-0.39\times10^{-3}\rho^2\mathcal{E}^2$	$1-0.25\times10^{-7}\rho^2\mathcal{E}^2$
$5s10s\ ^1S_0 \rightarrow 5s9p\ ^1P_1$	$1-0.10\times10^{-3}\rho^2\mathcal{E}^2$	$1-0.10\times10^{-3}\rho^2\mathcal{E}^2$	$1-0.14\times10^{-5}\rho^2\mathcal{E}^2$
$5s11s\ ^1S_0 \rightarrow 5s10p\ ^1P_1$	$1-0.15\times10^{-3}\rho^2\mathcal{E}^2$	$1+0.41\times10^{-3}\rho^2\mathcal{E}^2$	$1-0.12\times10^{-5}\rho^2\mathcal{E}^2$
$5s12s\ ^1S_0 \rightarrow 5s11p\ ^1P_1$	$1-0.28\times10^{-3}\rho^2\mathcal{E}^2$	$1+0.20\times10^{-2}\rho^2\mathcal{E}^2$	$1-0.11\times10^{-5}\rho^2\mathcal{E}^2$

turbed eigenfunctions.

The dependence of λ, S, and N on the electric-field strength can be derived using (14), (17), and (19). Table IV shows the results for the investigated SF transitions of Sr. Based on the low electric-field strength in the experiments, the terms with power higher in $\mathcal{E}$ than $\mathcal{E}^2$ were neglected because they are several orders of magnitude smaller. The greatest contribution to the dependence of the maximum of the intensity of the SF pulse on the electric field (13) comes form the wavelength λ and the line strength S, whereas the contribution of N can be neglected (Table III). The same was found for the other elements. The contributions to the peak intensity for all theoretical models were derived with (13). The contributions beyond $\mathcal{E}^2$ were again neglected. In order to provide a comparison between the theoretical and experimental results, the gradient of the straight line relating $\sqrt{I_M(\mathcal{E})/I_M(\mathcal{E}=0)}$ and $\mathcal{E}^2$ is listed in Table II.

For the investigated transitions of Sr the theoretical results are not in agreement with experiment. However, this is not surprising because we have used the Coulomb approximation for the calculation of the radial integrals. From lifetime [22,23] and Stark-effect investigations [41] it is known that the Coulomb approximation for these levels is not a suitable method for calculating the radial integrals.

For the investigated transitions of Ba, Table II shows an agreement of the sign between experimental and theoretical gradients, but the theoretical values are two orders of magnitude too small for all the theoretical models. The reason for this difference might again be the Coulomb approximation [42].

For Na, however, the Coulomb approximation should be a good method for calculating the radial integrals [43–45]. Despite this, Table II shows only an agreement of the sign between experimental and theoretical gradients, whereas all the calculated values are too small.

CONCLUSION

The experiments reported in this paper demonstrate that superfluorescent transitions react very sensitively to external electric fields. Thus it is possible to suppress superfluorescent transitions by applying field with strengths lying between several tens of V/cm and several kV/cm, depending on the investigated element and transition. It was found for all the investigated superfluorescent transitions that the square root of the maximum of the intensity of the superfluorescent pulse decreases linearly with the square of the electric-field strength. This is confirmed for most transitions by calculations using different theoretical models.

ACKNOWLEDGMENTS

We would like to thank Professor Dr. A. Steudel for his interest in this work and helpful discussions. We are indebted to the Regionales Rechenzentrum für Niedersachsen for making computer facilities available. This work was supported by the Deutsche Forschungsgemeinschaft.

[1] R. H. Dicke, Phys. Rev. **93**, 99 (1954).
[2] N. Skribanowitz, I. P. Herman, J. C. MacGillivray, and M. S. Feld, Phys. Rev. Lett. **30**, 309 (1973).
[3] R. Bonifacio and L. A. Lugiato, Phys. Rev. A **11**, 1507; **12**, 587 (1957).
[4] H. M. Gibs, Q. H. F. Vrehen, and H. M. J. Hickspoors, Phys. Rev. Lett. **39**, 547 (1977).
[5] *Cooperative Effects in Matter and Radiation,* edited by C. M. Bowden, D. W. Howgate, and H. R. Robl (Plenum, New York, 1977).
[6] A. T. Rosenberger, S. J. Petuchowski, and T. A. DeTemple, Ref. 5, p. 15.
[7] M. Gross, C. Fabre, P. Pillet, and S. Haroche, Phys. Rev. Lett. **36**, 1035 (1976).
[8] A. Flusberg, T. Mossberg, and S. R. Hartmann, Ref. 5, p. 37.
[9] A. Crubellier, S. Liberman, and P. Pillet, Phys. Rev. Lett. **41**, 1237 (1978).
[10] C. Brechignac and P. Cahuzac, J. Phys. (Paris) Lett. **40**, L123 (1979).
[11] P. Cahuzac, H. Sonntag, and P. E. Toschek, Opt. Commun. **31**, 37 (1979).
[12] P. Kulina, C. Leonard, and R.-H. Rinkleff, Phys. Rev. A **34**, 227 (1986).
[13] L. Moi, P. Goy, M. Gross, J. M. Raimond, C. Fabre, S. Haroche, Phys. Rev. A **27**, 2043 (1983).
[14] P. Goy, L. Moi, M. Gross, J. M. Raimond, C. Fabre, and S. Haroche, Phys. Rev. A **26**, 2065 (1982).
[15] T. Becker, R.-H. Rinkleff, and A. Steudel, Appl. Phys. B **49**, 257 (1989).
[16] F. T. Arecchi and E. Courtens, Phys. Rev. A **2**, 1730 (1970).

[17] R. Friedberg and S. R. Hartmann, Phys. Rev. A **13**, 495 (1976).
[18] R. E. Slusher and H. M. Gibbs, Phys. Rev. A **5**, 1634 (1972).
[19] W. A. Molander and C. R. Strout, J. Phys. B **15**, 2109 (1982).
[20] N. E. Rehler and J. H. Eberly, Phys. Rev. A **3**, 1735 (1971).
[21] M. S. Feld and J. C. MacGillivray, in *Coherent Nonlinear Optics,* edited by M. S. Feld and V. S. Letokhov (Springer, Berlin, 1980), p. 7.
[22] W. Gornik, Z. Phys. A **283**, 231 (1977).
[23] G. Jönsson, C. Levinson, A. Persson, and C. G. Wahlström, Z. Phys. A **316**, 255 (1984).
[24] D. R. Bates and A. Damgaard, Philos. Trans. R. Soc. London **242**, 101 (1949).
[25] H. Friedrich, K. Katterbach, and E. Trefftz, J. Quant. Spectrosc. Radiat. Transfer **10**, 11 (1970).
[26] T. Becker, Doctoral thesis, Universität Hannover, 1989.
[27] R. Saunders and R. H. Bullough, Ref. 5, p. 209.
[28] P. Kulina and R.-H. Rinkleff, Z. Phys. A **318**, 251 (1984).
[29] J. R. P. Angel and P. G. H. Sandars, Proc. R. Soc. London, Ser. A **305**, 125 (1968).
[30] J. P. Rubbmark and S. A. Borgström, Phys. Scr. **18**, 196 (1978).
[31] P. Esherick, Phys. Rev. A **15**, 1920 (1977).
[32] R. Beigang, K. Lücke, A. Timmermann, P. J. West, and D. Frölich, Opt. Commun. **42**, 19 (1982).
[33] K. T. Lu, J. Opt. Soc. Am. **64**, 706 (1974).
[34] K. T. Lu, Proc. R. Soc. London, Ser. A **353**, 431 (1977).
[35] M. Aymar, P. Camus, M. Dieulin, and C. Morillon, Phys. Rev. A **18**, 2173 (1978).
[36] J. A. Armstrong, J. J. Wynne, and P. Esherick, J. Opt. Soc. Am. **69**, 211 (1979).
[37] J. R. Rubbmark, S. A. Borgström, and K. Bockasten, J. Phys. B **10**, 421 (1977).
[38] P. Camus, M. Dieulin, and A. El. Himdy, Phys. Rev. A **26**, 379 (1982).
[39] C. E. Moore, *Atomic Energy Levels,* Natl. Bur. Stand. Ref. Data Ser., Natl. Bur. Stand. (U.S.) Circ. No. 35 (U.S. GPO, Washington, D.C., 1971), Vol. I.
[40] M. Aymar and O. Robaux, J. Phys. B **12**, 531 (1979).
[41] T. Becker and R.-H. Rinkleff, Arabian J. Sci. Eng. **13**, 203 (1988).
[42] D. Kaiser, P. Kulina, A. E. Livingston, H.-H. Radloff, and S. Tudorache, Z. Phys. A **285**, 111 (1978).
[43] D. Kaiser, Phys. Lett. **51A**, 375 (1975).
[44] T. F. Gallagher, S. A. Edelstein, and R. M. Hill, Phys. Rev. A **11**, 1504 (1975).
[45] R. T. Hawkins, W. T. Hill, F. V. Kowalski, A. L. Schawlow, and S. Svanberg, Phys. Rev. A **15**, 967 (1977).